Frequency-dependency of force dynamics in hybrid reluctance actuators

Christian Haider, Ernst Csencsics, and Georg Schitter

***Abstract*—In this paper, the dynamics of hybrid reluctance actuators (HRAs) are investigated by conducting dynamic force measurements on two HRAs, one with a laminated core and one with a solid core. The performance of current-controlled HRAs is limited by a frequency-dependent force-to-current relationship (FCR), which leads to a higher current demand for a constant force generation at higher frequencies due to eddy current diffusion in the stator yoke. The FCR is further depending on the amplitude of the driving signal due to hysteresis. Flux feedback control on the other hand can realise a largely frequency-independent force-to-flux relationship (FFR) up to 1 kHz for both a solid and a laminated core actuator. The force dynamics are evaluated in the frequency domain and the power consumption for positioning applications is compared for a current-controlled layered core and a flux-controlled solid core HRA, showing an increased power consumption by a factor of six in the latter case.**

I. Introduction

In modern industrial environments, there is a critical demand for high-precision motion control, particularly in sectors such as manufacturing and metrology [1]. For precise positioning in the nanometer range, piezoelectric actuators are commonly used [2]. For larger actuation ranges, electromagnetic voice coil actuators (VCAs), utilizing the Lorentz force are preferred due to their high linearity [3]. Their characteristic zero-stiffness property ensures a position-independent force generation, which is beneficial for vibration isolation systems. These actuators are integral to systems ranging from precision machining [4] and multiaxis scanning devices [5] to fast steering mirrors (FSMs) [6], [7] and active sample-tracking measurement platforms [8]. However, a notable limitation of VCAs is their relatively small motor constant (force-to-current ratio), requiring high currents for the necessary high acceleration and leading to resistive heating, which can produce a large temperature gradient [9]. Reluctance actuators offer a quadratic force-to-current relationship and can achieve higher force density with less heat dissipation but face challenges such as non-linear force-to-current relations, magnetic hysteresis, and high position-dependence [10], [11].
By adding a permanent magnet, hybrid reluctance actuators (HRAs) are obtained, where the coil flux is superimposed with the bias flux of the permanent magnet in a ferromagnetic yoke [12]. This presents a promising advancement by enabling a linear force-to-current relationship and a motor constant several times higher than traditional VCAs [12]. HRAs are used in applications like FSMs [13], tool servos [14], vibration isolation systems [15] and zero-power gravity compensation systems [16] but they still encounter the challenge of position-dependent force and inherent non-linearities such as magnetic hysteresis and eddy currents [17], [18]. To address these nonlinearities, strategies such as utilizing materials with high permeability and electric resistance or manufacturing yokes from laminated steel sheets have been explored [17], [19]. In laminated-core HRAs, performance limitations are encountered if the yoke cross section is reduced. The effective fill factor decreases and thus less flux can be guided through the yoke, limiting the achievable force and motor constant of the actuator. Previous work compares the dynamics of a solid and laminated core HRA, showing that flux control allows for extending the positioning bandwith of a solid core HRA by a factor of 10 compared to current control [20].
The contribution of this paper is the comparison of HRA dynamics in dependence of control scheme and core configuration together with the realization of a frequency independent force generation demonstrated by dynamic force measurements.

The authors are at the Automation and Control Institute (ACIN), TU Wien, Gusshausstrasse 27-29, 1040 Vienna, Austria. Corresponding author: haider@acin.tuwien.ac.at

II. System modelling

The operation of a hybrid reluctance actuator involves the interaction of two types of magnetic fluxes: the magnetic bias flux Φ_m created by a permanent magnet and the coil flux Φ_c generated by two actuation coils connected in series. The bias flux establishes a proportional relationship between the coil current I and the actuation force F generated by the actuator. The working principle is depicted in Fig. 1.
By analysing the parallel magnetic circuit of the HRA, the fluxes across the left and right air gap can be derived as

$$\Phi_l = \Phi_c + \Phi_m \frac{R_r}{R_l + R_r} = \Phi_v + \frac{1}{2}\Phi_m \tag{1}$$

$$\Phi_r = \Phi_c - \Phi_m \frac{R_l}{R_l + R_r} = \Phi_v - \frac{1}{2}\Phi_m \tag{2}$$

with the air gap reluctances R_l, R_r and R_f. Splitting the fluxes into a constant part Φ_m and a variable component Φ_v [18] with

$$\Phi_v = \Phi_c + \Phi_m \frac{x}{2x_g}, \tag{3}$$

allows for deriving a linear force-to-flux relationship (FFR)

$$F = \frac{\Phi_l^2 - \Phi_r^2}{2\mu_0 A} = \frac{1}{2\mu_0 A}\Phi_m \Phi_v = K_{m\Phi}\Phi_v, \tag{4}$$

Post-print version of the article: C. Haider, E. Csencsics, and G. Schitter, "Frequency-dependency of force dynamics in hybrid reluctance actuators," *2024 IEEE International Conference on Advanced Intelligent Mechatronics (AIM)*, 2024.
DOI: 10.1109/AIM55361.2024.10637132

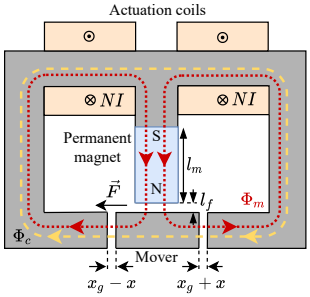

Fig. 1: Working principle of a hybrid reluctance actuator. The coil current determines the mover displacement.

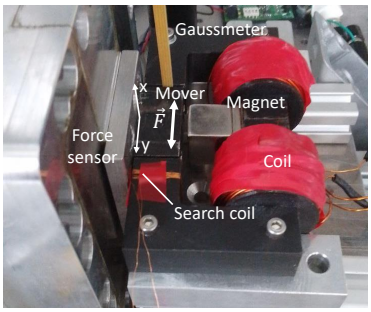

Fig. 2: Experimental setup of the solid core HRA with the mover directly mounted to the force sensor via an aluminium adapter. For the laminated core HRA, the solid yoke is exchanged by a stack of laminated steel sheets. The mover actuation direction is parallel to the force sensor's y-axis. A Gaussmeter is inserted in the air gap to measure the air gap flux.

with the motor constant $K_{m\Phi}$ by using the Maxwell stress tensor [21]. Using Ampere's circuital law, the coil flux calculates to

$$\Phi_c = \frac{2NI}{R_l + R_r}, \tag{5}$$

and the permanent magnet's flux can be obtained via

$$\Phi_m = \frac{H_c l_m}{R_m + R_f + \frac{R_l R_r}{R_l + R_r}} \tag{6}$$

with the permanent magnet's coercivity H_c. By substituting for Φ_m and Φ_v, the force equation can also be written as

$$F = K_{mI}(x)I + k_a(x)x \tag{7}$$

showing the force-to-current relationship (FCR) with a position-dependent motor constant $K_{mI}(x)$ and an actuator stiffness $k_a(x)$ [18].

III. System Design

The experimental setup for the force measurement of the HRA is depicted in Fig. 2. For the solid core, a solid steel yoke (EN10025-S235JR) is used. For the layered core HRA experiments, the solid yoke is exchanged by a stack of 29 steel sheets of the same type. Two identical actuation coils are connected in series and attached to a custom-made power

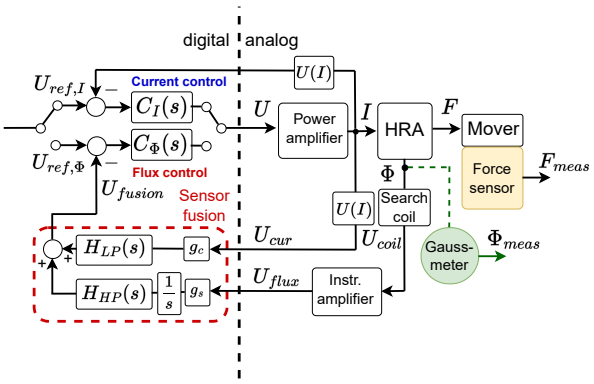

Fig. 3: Control structure for both actuator setups. Either flux or current controllers are activated to perform force measurements. The gaussmeter is used for reference measurements in the air gap.

amplifier with an integrated shunt resistor to measure the coil current. The ferromagnetic mover is rigidly attached to the vertically mounted force sensor (K3D120-500N, ME-Messsysteme, Germany) via an adapter plate. Therefore, the nominal moving range of about 2 mm is reduced for the force measurements. The measured voltage across the bridge circuit of the strain gauges is amplified by a commercial amplifier (GSV-1A4, ME-Messsysteme) with a sensitivity of 5.99 N/V. In order to enable a flux measurement, the induced voltage in a search coil is measured and amplified with an instrumentation amplifier (INA126U, Texas Instruments, USA). The induced voltage is integrated in order to derive the magnetic flux linkage. To prevent the integration of low-frequent noise, a sensor fusion structure, consisting of a low pass filter for the measured coil current and a high pass filter for the integrated search coil signal is implemented, as depicted in Fig. 3.
For reference measurements, a gaussmeter probe (G-08, Hirst Magnetics, UK) is inserted in the mover airgap and the flux density is measured. The measured flux and current signals are read via 16-bit ADCs connected to a field-programmable gate array (FPGA) (DS5203, dSpace GmbH, Germany) with a sampling frequency of 10 MHz. The specifications of the setup are summarized in Tab. I.

TABLE I: Dimensions of both experimental actuators.

Parameter	Symbol	Value
Cross-section area	A	15 mm × 15 mm
Coercitivity	H_c	1 MA/m
Air gaps	x_g, l_f	1 mm
Magnet length	l_m	19 mm
Coil windings	N	120
Search coil windings	N_{coil}	16
Sheet thickness	d	0.5 mm

Post-print version of the article: C. Haider, E. Csencsics, and G. Schitter, "Frequency-dependency of force dynamics in hybrid reluctance actuators," *2024 IEEE International Conference on Advanced Intelligent Mechatronics (AIM)*, 2024.
DOI: 10.1109/AIM55361.2024.10637132

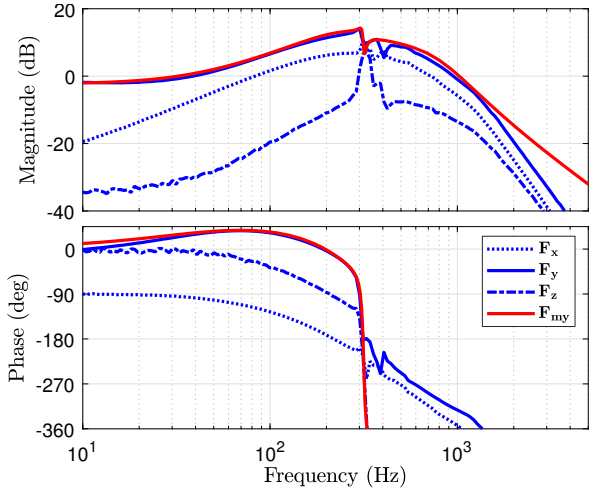

Fig. 4: Dynamic force measurement of the flux-controlled solid core HRA. The mover is actuated parallel to the y-axis and F_y shows the dominant contribution. F_{my} represents the modelled force sensor dynamics for this measurement.

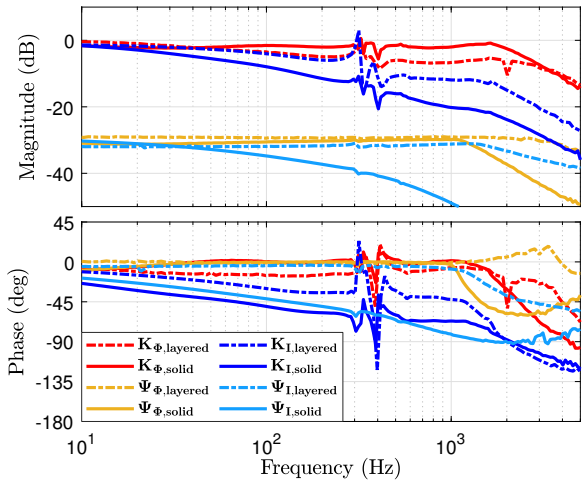

Fig. 5: Dynamic force measurement (divided by the modelled dynamics F_{my}) comparison with current and flux control for both actuators, respectively. $K_{\Phi,\text{layered}}$ and $K_{\Phi,\text{solid}}$ show the measured FFR for flux control for both HRAs, showing a relatively constant force generation up to about 2 kHz. The measured fluxes in the air gap underline these measurements, as the generated flux stays constant for about the same bandwidth. $K_{I,\text{layered}}$ and $K_{I,\text{solid}}$ depict the FCRs of the current controlled actuators, both showing a decreasing trend with rising frequency.

A. Control structure

In order to compare both actuator types, current and flux controllers are implemented on the rapid prototyping system. The PI-controllers of the form

$$C_{PI} = k_p + \frac{k_i}{s} \tag{8}$$

are designed for the current and flux control for the layered core and for the current control of the solid core.
For the flux-controlled solid core, a PID-controller of the form

$$C_{PID} = k_p + \frac{k_i}{s} + k_d \frac{s}{T_f s + 1} \tag{9}$$

is implemented, as eddy current diffusion leads to a larger phase lag in the solid core and an additional differentiating action is needed [20]. The additional pole with $T_f = 1.989 \times 10^{-5}$ and $k_d = 8.442 \times 10^{-4}$ is added to limit the differentiating action at higher frequencies. The controllers of both systems are designed to show a similar closed loop bandwidth of about 8 kHz. The control parameters and the phase and gain margins are shown in Tab. II.

TABLE II: Control parameters for both actuators with gain and phase margins.

	$C_{I,\text{solid}}$	$C_{I,\text{layered}}$	$C_{\Phi,\text{solid}}$	$C_{\Phi,\text{layered}}$
k_p	21.877	70.794	46.901	6.309
k_i	2.749×10^5	4.448×10^5	1.122×10^5	3.964×10^4
GM	11.2 dB	16.3 dB	6.2 dB	12 dB
PM	60°	52°	35°	47°

IV. Experimental Results

In order to compare the electromagnetic force generation of both actuator types for current control and flux control, respectively, transfer functions are measured up to 5 kHz from the respective reference to the output of the force sensor, F_{meas}. For a concise comparison, the terms force-to-flux relationship (FFR) and force-to-current relationship (FCR) introduced in Eq. 4 and Eq. 7 are used in the following.

A. Force measurements

First, a measurement is conducted for the flux-controlled solid core actuator, with results depicted in Fig. 4. While the y-axis is the principal axis of actuation (see Fig. 2), the additional axes also contribute to the overall force of the actuator. A reason for this effect could be a undulated displacement of the mover due to variations in the mounting screw torque and an imperfect attachment to the force sensor. The shown dynamics of F_y make it difficult to compare the two actuators and the two control principles with each other. As a remedy, the force sensor dynamics of the flux-controlled solid core actuator are modelled as a 6th order system F_{my}. By dividing the force measurements by F_{my}, this model sets a baseline and enables a comparative analysis of the four HRA configurations.
In Fig. 5, the resulting transfer functions of the dynamic force measurements for the solid and the layered core actuator with active current and flux control, measured from flux and current reference to the force sensor signal, are depicted. For current control, the FCR of the solid core, $K_{I,\text{solid}}$ indicates a decline of about -10 dB per decade, resulting from eddy current diffusion in the solid yoke. As a consequence, the decreasing flux density impairs the force generation. This is validated by the Gaussmeter measurement $\Psi_{I,\text{solid}}$ in the left air gap which

Post-print version of the article: C. Haider, E. Csencsics, and G. Schitter, "Frequency-dependency of force dynamics in hybrid reluctance actuators," *2024 IEEE International Conference on Advanced Intelligent Mechatronics (AIM)*, 2024.
DOI: 10.1109/AIM55361.2024.10637132

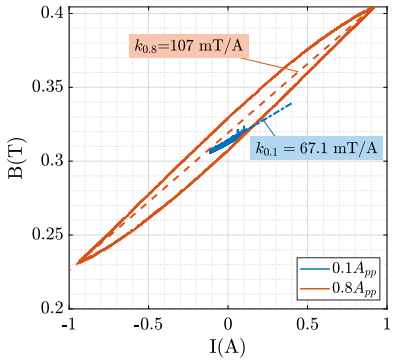

Fig. 6: Measured hysteresis curves of the current controlled solid core HRA for driving signals with amplitudes $0.1A_{pp}$ and $0.8A_{pp}$, respectively.

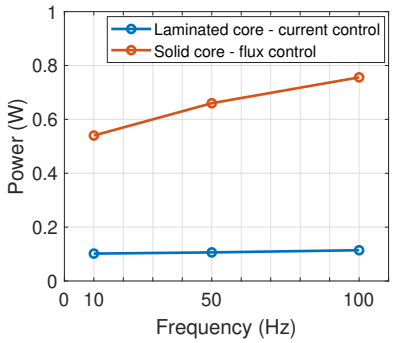

Fig. 7: Power consumption for both actuator types. Each HRA is actuated at the drive frequencies 10, 50 and 100 Hz with active position control to allow for a fair comparison. A sinusoidal position reference signal with an amplitude of 20 µm is used for all measurements.

also shows a significant decrease in the measured flux density. Compared to that, $\Psi_{I,\text{layered}}$ shows a relatively constant flux magnitude up to 1 kHz, resulting from the eddy current inhibition due to the layered core. The corresponding force transfer function $K_{I,\text{layered}}$ shows a decrease of -6 dB in the range from 10 Hz to 100 Hz. Here it has to be noted, that the mounting of the layered mover is not as trivial as with the solid version, possibly impairing this measurement result. However, the flux-controlled version shows further improvement, as the FFR of $K_{\Phi,\text{layered}}$ shows a decrease of only -2 dB in the 10-100 Hz range. The flux-controlled solid core $K_{\Phi,\text{solid}}$ shows a largely constant FFR up to almost 2 kHz.

B. Hysteresis

It is essential to point out that the force measurements reflect only the differences between the two actuator cores and the respective control schemes, since the transfer functions are normalized to $K_{\Phi,\text{solid}}$ by dividing them by F_{my}. Comparing the flux controlled actuators, it can be seen that both actuator cores can deliver a relatively constant force magnitude up to about 1 kHz, whereas the current controlled actuators suffer from a decreasing force magnitude. Additionally, hysteresis influences the magnetic field generation in current-controlled actuators, as the resulting non-linearities are not captured by current feedback control. The motor constant is therefore dependent on the driving frequency and the current amplitude. This can be seen by investigating the hysteresis of the actuator yoke.

The hysteresis of the current-controlled solid core HRA, depicted in Fig. 6, is measured using a 0.1 Hz reference current with an amplitude of 0.1 A and 0.8 A, respectively. For 0.1 A, the gradient of the hysteresis curve shows a slope of 67 mT/A, which increases to 107 mT/A for the higher amplitude of 0.8 A, directly impairing the motor constant in the current-controlled case. This means a smaller current produces a weaker magnetic field, which is not strong enough to re-orientate the majority of the magnetic domains in the actuator. Thus, less flux is available for electromagnetic force generation and hence the motor constant is smaller. For a DC current of 0.5 A, the nominal motor constant calculates to $K_{mI} = 18\,\text{N/A}$ for both actuators and changes for varying current amplitudes.

With flux control, the non-linearities arising from hysteresis and eddy currents are captured in the flux measurement by the search coil and hence the varying reference signal amplitude does not influence the resulting motor constant. For a DC current of 0.5 A, corresponding to a variable flux density of $B_v = \Phi_v/A = 48\,\text{mT}$ in the air gap, the motor constant results to $K_{mB} = 75\,\text{N/T}$, which does not change for varying reference amplitudes.

C. Energy efficiency

In order to evaluate the power consumption of both actuator types, the current and the voltage at the power amplifier's terminals are measured for both actuators. For a fair comparison, position controllers are implemented for the current-controlled layered core and the flux-controlled solid core actuator, as described in [20]. The movers are detached from the force sensor and guided by an aluminium flexure, adding a positive stiffness to the HRA systems, rendering them open-loop stable around the center [18]. The mover motion is observed with an interferometric sensor and a cascaded control structure is implemented, resulting in a closed-loop bandwidth of 790 Hz for the current-controlled layered core and 750 Hz for the flux-controlled solid core [20]. A sinusoidal reference with an amplitude of 50 µm is tracked for the driving frequencies 10 Hz, 50 Hz and 100 Hz for both actuators, as depicted in Fig. 7.

For the solid core, the power consumption is higher by a factor of 6 when tracking a 10 Hz reference. Compensating the field-weakening effects of the induced eddy currents necessitates a higher voltage at the actuator coils and thus a higher power consumption. Eddy current losses in the yoke increase quadratically with the frequency, while hysteresis losses linearly depend on the frequency. The two aspects contribute to the overall power demand and together with the amplitude-dependent hysteresis in the current-controlled case, make it difficult to distinguish the effects in Fig. 7. In the laminated actuator,

Post-print version of the article: C. Haider, E. Csencsics, and G. Schitter, "Frequency-dependency of force dynamics in hybrid reluctance actuators," *2024 IEEE International Conference on Advanced Intelligent Mechatronics (AIM)*, 2024.
DOI: 10.1109/AIM55361.2024.10637132

yoke layering inhibits eddy current formation to an extent and consequently the power consumption stays roughly constant. In summary, the force dynamics of four HRA configurations are analysed, where the implemented flux control enables an approximately frequency-independent force generation up to 1 kHz for both actuator cores with a six-fold higher energy consumption in the solid core configuration.

V. Conclusion

This paper compares the dynamics of force generation in hybrid reluctance actuators for different HRA control schemes and core configurations. Implementing flux feedback control ensures a linear force output across a broad frequency range, up to 1 kHz, largely independent of the core configuration. With current control, the solid core HRA shows a -10 dB per decade decline in the force-to-current relationship, directly resulting from eddy current diffusion. With yoke layering, the actuator shows a relatively constant flux generation up to 1 kHz, also showing in the force dynamics. Due to hysteresis, the force-to-current ratio is amplitude-dependent, which can only be marginally compensated by yoke layering, as opposed to the flux controlled case. The power consumption is evaluated for the solid core HRA with flux control and compared to a layered core with conventional current control, showing a six-fold higher energy consumption for the solid core HRA for the same driving frequency of 100 Hz.

References

[1] Z. Zhang, H. Zhou, and J.-a. Duan, "Design and analysis of a high acceleration rotary-linear voice coil motor," *IEEE Transactions on Magnetics*, vol. 53, no. 7, pp. 1–9, 2017.

[2] F. R. Leiro, A. Bazaei, S. Regnier, and M. Boudaoud, "Feedback control strategy for a high speed differential piezo-driven stage by an exclusive use of piezoelectric sensors," in *2022 American Control Conference (ACC)*, DOI 10.23919/ACC53348.2022.9867360, pp. 4389–4396, 2022.

[3] B. Black, M. Lopez, and A. Morcos, "Basics of voice coil actuators," *PCIM-VENTURA CA-*, vol. 19, pp. 44–44, 1993.

[4] Q. Xu, "Design and implementation of a novel rotary micropositioning system driven by linear voice coil motor," *Review of Scientific Instruments*, vol. 84, no. 5, p. 055001, May. 2013.

[5] D. Kang, K. Kim, D. Kim, J. Shim, D.-G. Gweon, and J. Jeong, "Optimal design of high precision xy-scanner with nanometer-level resolution and millimeter-level working range," *Mechatronics*, vol. 19, no. 4, pp. 562–570, 2009.

[11] A. Katalenic, H. Butler, and P. P. J. van den Bosch, "High-precision force control of short-stroke reluctance actuators with an air gap observer," *IEEE/ASME Transactions on Mechatronics*, vol. 21, no. 5, pp. 2431–2439, 2016.

[6] E. Csencsics and G. Schitter, "System design and control of a resonant fast steering mirror for lissajous-based scanning," *IEEE/ASME Transactions on Mechatronics*, vol. 22, no. 5, pp. 1963–1972, 2017.

[7] T. Shinshi, D. Shimizu, K. Kodeki, and K. Fukushima, "A fast steering mirror using a compact magnetic suspension and voice coil motors for observation satellites," *Electronics*, vol. 9, no. 12, p. 1997, 2020.

[8] D. Wertjanz, E. Csencsics, and G. Schitter, "3 dof vibration compensation platform for robot-based precision inline measurements on free-form surfaces," *IEEE Transactions on Industrial Electronics*, pp. 1–1, 2021.

[9] D. B. Hiemstra, G. Parmar, and S. Awtar, "Performance tradeoffs posed by moving magnet actuators in flexure-based nanopositioning," *IEEE/ASME Transactions on Mechatronics*, vol. 19, pp. 201–212, 2014.

[10] N. H. Vrijsen, J. W. Jansen, and E. A. Lomonova, "Comparison of linear voice coil and reluctance actuators for high-precision applications," in *Proceedings of 14th International Power Electronics and Motion Control Conference EPE-PEMC 2010*, pp. S3–29–S3–36, 2010.

[12] R. M. Schmidt, G. Schitter, A. Rankers, and J. Van Eijk, *The Design of High Performance Mechatronics: High-Tech Functionality by Multidisciplinary System Integration*, 2nd ed. IOS Press, 2014.

[13] E. Csencsics, J. Schlarp, and G. Schitter, "High-performance hybrid-reluctance-force-based tip/tilt system: Design, control, and evaluation," *IEEE/ASME Transactions on Mechatronics*, vol. 23, no. 5, pp. 2494–2502, 2018.

[14] D. Wu, X. Xie, and S. Zhou, "Design of a normal stress electromagnetic fast linear actuator," *IEEE Transactions on Magnetics*, vol. 46, no. 4, pp. 1007–1014, 2010.

[15] S. Ito, B. Lindner, and G. Schitter, "Sample-tracking vibration isolation with hybrid reluctance actuators for inline metrology," *IFAC-PapersOnLine*, vol. 52, no. 15, pp. 537–542, 2019.

[16] G. Stadler, E. Csencsics, S. Ito, and G. Schitter, "High precision hybrid reluctance actuator with integrated orientation independent zero power gravity compensation," *IEEE Transactions on Industrial Electronics*, vol. 69, DOI 10.1109/TIE.2021.3137444, no. 12, pp. 13 296–13 304, 2022.

[17] E. Csencsics, J. Schlarp, and G. Schitter, "Bandwidth extension of hybrid-reluctance-force-based tip/tilt system by reduction of eddy currents," in *2017 IEEE International Conference on Advanced Intelligent Mechatronics (AIM)*, pp. 1167–1172, 2017.

[18] S. Ito, F. Cigarini, and G. Schitter, "Flux-controlled hybrid reluctance actuator for high-precision scanning motion," *IEEE Transactions on Industrial Electronics*, vol. 67, no. 11, pp. 9593–9600, Nov. 2020.

[19] S. K. Mukerji, M. George, M. B. Ramamurthy, and K. Asaduzzaman, "Eddy currents in solid rectangular cores," vol. 7, pp. 117–131, 2008.

[20] C. Haider, E. Csencsics, and G. Schitter, "Analyzing the dynamic performance of hybrid reluctance actuators for feedback control," in *2024 IEEE/ASME International Conference on Advanced Intelligent Mechatronics (AIM)*, 2024, submitted.

[21] D. J. Kluk, M. T. Boulet, and D. L. Trumper, "A high-bandwidth, high-precision, two-axis steering mirror with moving iron actuator," *Mechatronics*, vol. 22, no. 3, pp. 257–270, Apr. 2012.

Post-print version of the article: C. Haider, E. Csencsics, and G. Schitter, "Frequency-dependency of force dynamics in hybrid reluctance actuators," *2024 IEEE International Conference on Advanced Intelligent Mechatronics (AIM)*, 2024.
DOI: 10.1109/AIM55361.2024.10637132